ABSTRACT

Title of Document: GEOMETRICAL RELATIONSHIPS SPECIFYING THE PHYLLOTACTIC PATTERN OF AQUATIC PLANTS.

Wanda Jean Kelly, Master of Science, 2008

Directed By: Professor Todd J. Cooke.
Cell Biology and Molecular Genetics.

Aquatic plants provide an opportunity to characterize the geometrical relationships of leaf patterning. A new polar-coordinate model was used to correlate meristem shape and leaf arrangement in aquatic plants. In aquatic plants, the primary geometrical relationship specifying spiral vs. whorled phyllotaxis is primordial position: primordia arising on the apical dome (as defined by displacement angles $\theta \leq 90°$ during maximal phase) are often positioned in spiral patterns, whereas primordia arising on the subtending axis (as defined by displacement angles of $\theta \geq 90°$ during maximal phase) are arranged in whorled patterns. A secondary geometrical relationship shows an inverse correlation between the primordial size : available space ratio and the magnitude of the Fibonacci numbers in spiral phyllotaxis or the number of leaves per whorl in whorled phyllotaxis. This geometrical analysis provides the morphological context for interpreting phyllotaxis mutants and for constructing realistic models phyllotactic patterns.

GEOMETRICAL RELATIONSHIPS SPECIFYING THE PHYLLOTACTIC PATTERN OF AQUATIC PLANTS

By

Wanda Jean Kelly.

Thesis submitted to the Faculty of the Graduate School of the
University of Maryland, College Park, in partial fulfillment
of the requirements for the degree of
Master of Science
2008

Advisory Committee:

Professor Todd J. Cooke, Chair
Associate Professor Caren Chang
Associate Professor Zhongchi Liu

Dedication

This thesis is dedicated to all those educators, from kindergarten to graduate school, whose efforts afford students of all ages the opportunity to become more than they themselves might have dreamt.

Acknowledgements

I can’t express enough thanks to Dr. Todd Cooke for his mentorship and friendship throughout my graduate career. Thank you also to my committee members, Dr. Caren Chang and Dr. Zhongchi Liu who freely offered their support and assistance.

I would like to thank the following people who contributed plants or provided the location of various species in the field: Dr. M. Stephen Ailstock, Anne Arundel Community College; Carl Anderson, International Society of Oleander; Susan Aufieri, aquarium hobbyist; Craig Aumack and Dr. Kenneth H. Dunton, University of Texas at Austin; Ron Dean and Dr. Michael J. Durako, University of North Carolina, Wilmington; Lisa Huey and Dr. William T. Haller, University of Florida, Gainesville; Dr. Kent Mountford, Cove Corporation; Mike Naylor, Maryland Department of Natural Resources; Dr. Christopher Preston, Center for Ecology and Hydrology, Monks Wood, UK. I also thank Dr. John Free, Eastern Nazarene College, and Dr. Donald R. Kaplan, University of California, Berkeley, for their constructive review of various manuscripts leading to this thesis.

Table of Contents

List of Tables

List of Figures

Chapter 1: Introduction and Background

Aquatic Angiosperms

Aquatic angiosperms have fascinated botanists for over 400 yr (Dodoens, 1578; Arber, 1920; Sculthorpe, 1967). Recent phylogenetic analyses of angiosperm evolution have identified the fossil aquatic plant family Archaefructaceae as the sister group to all angiosperms (Sun et al., 2002) and several living aquatic plants, including *Ceratophyllum*, *Cabomba* and *Potamogeton*, as having arisen from early divergent angiosperm lineages (Qiu et al., 2001). Moreover, terrestrial angiosperms have re-invaded aquatic environments a minimum of 205 times (Cook, 1970, 1999). Aquatic plants adopt an exceptional range of habits including submerged, floating, and emergent shoots with or without roots anchored into the substrate. Thus, aquatic angiosperms manifest the ability of the angiosperm lineage to evolve developmental innovations in response to ecological selection pressures. The underlying assumption of this thesis is that aquatic angiosperms are also expressing the complete range of different phyllotaxes (leaf arrangements). Therefore, I anticipate that aquatic plants may be especially useful for elucidating the basic geometrical relationships specifying phyllotactic patterning.

The initial phyllotactic pattern is established with the positioning of leaf primordia on the surface of the shoot apical meristem (Lyndon, 1998). This pattern may persist to form the observed arrangement of mature leaves, or it may be altered to develop a new pattern as the consequence of differential growth of various subapical regions. Three general

patterns are routinely observed on mature shoots: alternate (one leaf inserted at the node), opposite (two leaves), and whorled (three or more leaves). Alternate phyllotaxis, which is the most common pattern observed on the shoot tips of terrestrial plants, is routinely described in terms of the spirals of leaf primordia radiating from the meristem center (Erickson, 1983; Jean, 1992, 1994). If leaves are assigned a number in the order of their origin, then the intervals in leaf numbers between successive leaves on these spirals can typically be related to the enigmatic Fibonacci number series. However, the underlying causes of phyllotactic patterning remain elusive despite research into plausible chemical gradients (Thornley, 1975; Veen and Lindenmayer, 1977; Meinhardt, 1982), biomechanical stresses (Green et al., 1996; Green, 1999) and molecular regulation (Leyser and Furner, 1992; Clark et al., 1997; Itoh et al., 2000) operating in the shoot apical meristem.

A new geometrical model of phyllotaxis

In this thesis, a geometric approach was used to characterize the phyllotactic patterns in aquatic plants having Fibonacci spirals and non-Fibonacci whorls because previous biomechanical and biochemical models for phyllotactic patterning were largely divorced from the fundamental geometry of the meristems responsible for these patterns. Using a polar-coordinate model of shoot apical meristems, I have discovered striking geometric relationships between the positions of new primordia and the resulting phyllotaxis. These new insights may help to separate the underlying mechanism of leaf positioning from the more specialized process of primordial initiation in Fibonacci spirals. Moreover, these geometric relationships may provide the structural context for the expression of molecular mechanisms involved in leaf initiation.

Chapter 2: Material and Methods

Aquatic Plant Survey

Angiosperm characteristics were surveyed by using the data retrieval program Intkey to analyse The Families of Flowering Plants, a Delta (DEscription Language for TAxonomy) database (Dallwitz et al., 2000; Watson and Dallwitz, 2000). The advanced mode was chosen to screen 583 angiosperm families. Settings were changed from the default settings to those recommended for data retrieval. The ecological type was set to hydrophyte to identify an initial list of angiosperm families with aquatic members and a second initial list of angiosperm families lacking aquatic members. The character of leaves-insertion was then used to screen for the presence of alternate, opposite, and whorled species in the families of the initial hydrophyte, initial nonhydrophyte, and total lists.

Various taxonomic sources (Cook, 1970; Gleason and Cronquist, 1991; Heywood, 1993; Zomlefer, 1994) were used to determine whether each hydrophyte family in the initial list had sufficient aquatic genera to warrant being considered a genuine hydrophyte family. Large families composed of more than 100 genera that were almost exclusively composed of terrestrial genera were eliminated from the initial hydrophyte list. Smaller families with aquatic species in 10% or less of their genera were also excluded from the final hydrophyte list. Lastly, families composed of a single genus with less than 10% aquatic species were also excluded. The leaf insertion data for the final hydrophyte list

were manually adjusted to reflect the exclusion of families from the initial list based on the criteria outlined. Similarly, those same families were manually added to the initial nonhydrophyte list for inclusion in the final nonhydrophyte list.

Apical Meristem Measurements

Using an Olympus SZH10 research stereoscope at magnifications up to 140X, 4–14 healthy shoots per species were hand-dissected (Table 1). The meristems were kept hydrated while enough leaves were carefully removed in order to expose the youngest primordium. The hydrated apices were transferred in depression slides to a Wild (Wild Heerbrugg Ltd., Heerbrugg, Switzerland) compound microscope where the apical domes and youngest primordia were drawn in sagittal view with a camera lucida at 200X. The image from a slide micrometer was also drawn to determine the magnification of the meristem images. When appropriate, enlarged copies of published median longitudinal sections of shoot apical meristems and supplemental textual descriptions were used to augment the live materials (Table 1).

Table 1. Plant sources and data collection methods.

Specimen name	Number of samples	Data collection	Source
Anacharis densa (=Elodea densa)	9	Hand dissection	Carolina Biological Supply
Anacharis densa	1	Literature	Savelkoul, 1957
Bacopa carolinia	6	Hand dissection	Pet Smart, Rockville, MD
Bacopa moneria	5	Hand dissection	Pet Smart, Rockville, MD
Cabomba sp.	7	Hand dissection	Carolina Biological Supply

Callitriche heterophylla	8	Literature	Deschamp and Cooke, 1985
Ceratophyllum densa.	14	Hand dissection	Carolina Biological Supply
Diantherea americana	2[a]	Literature	Sterling, 1949
Hippuris sp	7	Literature	McCully and Dale, 1961; O'Brien and McCully, 1969
Hydrilla sp	6	Hand dissection	Brookside Gardens, Wheaton, MD
Isoetes engelmannii	2[a]	Literature	Sam, 1984
Isoetes riparia	2[a]	Literature	Sam, 1984
Ludwigia pervensus	7	Hand dissection	Pet Smart, Rockville, MD
Myriophyllum aquatica	3	Hand dissection	Brookside Gardens, Wheaton, MD.
Myriophyllum heterophyllum	6	Literature	England and Tolbert, 1964
Myriopyllum spicatum	6	Hand dissection	Potomac River, Washington D.C
Najas quadalupensis	5	Hand dissection	Outdoor tank at University of Florida
Najas sp.	4	Hand dissection	Susan Aufieri's freshwater aquarium
Potamogeton perfoliatus	8	Hand dissection	Anne Arundel Community College
Proserpinanca palustris	4	Literature	Schmidt and Millington, 1968
Ranunculus flabellaris	5	Literature	Bostrack and Millington, 1962
Oryza sativa	8	Literature	Tamure et al. 1992; Matsuo and Hoshikawa, 1993; Nagasawa et al. 1996; Itoh et al. 1998
Rotalia indica	10	Hand dissection	Congressional Aquarium, Rockville MD
Zannachellia palustris	7	Hand dissection	Osborn Cove, Lusby, MD; Whitehurst Club, Severna Park, MD

a. These data were reported as minimal and maximal values and represent a larger sample taken by the previous authors

The apical tip was assumed to be symmetrical around a central axis and could be treated as the segment of a sphere, no larger than a hemisphere, on top of a cylinder or truncated cone. A best-fit circle was drawn to coincide very closely with the outline of each apical dome. In the case of convex meristems, this circle connected the highest point at the dome summit, the insertion point of the youngest primordium and the point opposite the insertion point on the other side of the apical dome (Fig. 1A).

Fig. 1. Polar-coordinate models for meristems of different shapes, as defined by their height-to-width ratios. (A) Convex meristem with h < w/2. (B) Concave meristem with h < 0. (C) Flat meristem with h = 0. (D) Elongated meristem with h > w/2. *h*, height; *r*, radius; *w*, width; *x*, linear displacement; θ, angular displacement

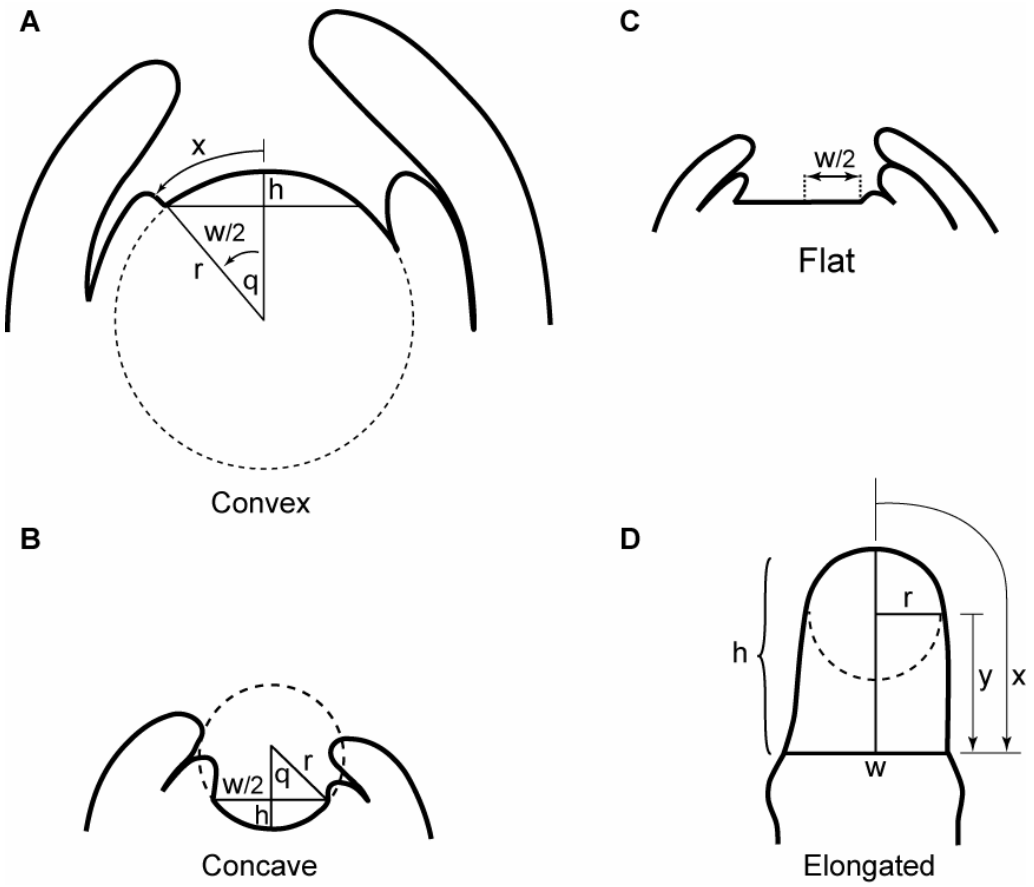

Based on elementary geometry, these three points in a nonlinear array must define one and only one circle. The width was then measured as the distance between the two opposite points, and the height was the perpendicular distance from the width line to the dome summit (Gifford, 1954). Using trigonometry, these height and width measurements were then converted to polar coordinates (Table 2).

Table 2. Definitions, calculations, and measurements for meristems with different shapes.

Meristem Shape	Definition	r	θ	x/r
A. Convex	w/2<h	$\frac{w^2 + 4h^2}{8h}$	arcsin (w/2r)	θπ/180
B. Concave	h< 0	$\frac{w^2 + 4h^2}{8h}$	arcsin (w/2r)	θπ/180
C. Flat	h= 0	∞	arcsin (w/2r)	0
D. Elongated	h>w/ 2	Measured	90°	(π/2) + (h-r)/r

The radius (*r*) of the shoot apex corresponded to the radius of the defined circle, and the position of the youngest leaf primordium was represented by the displacement angle (θ), which was delimited by the radius connecting the highest point on the dome summit and the radius drawn to the insertion point of the youngest primordium. The angular displacement (θ) was converted into a linear displacement (*x*) along the circle by multiplying the arc defined by theta and the circle circumference, or

$$x = (\theta/360)(2\pi r).$$

To normalize for meristems with different *r* values, this equation was rearranged to divide the linear displacement by the radius so that

$$x/r = \theta\pi/180$$

where x/r represents the normalized linear displacement (Table 2). Consequently, an angular displacement of zero ($\theta = 0°$) equated to an x/r of zero, and a θ of 90° would always yield an x/r of $\pi/2$ or 1.57.

This geometric model, originally derived for quantifying convex meristems, was modified for concave, flat, and elongated meristems (Fig. 1, Table 2). Concave meristems were treated the same as convex meristems except that their heights were recorded as negative numbers (Fig. 1B). For flat meristems, the heights were set at zero and their widths were measured as twice the distance from the meristem center to the insertion point of the youngest primordium (Fig. 1C). Their x values were arbitrarily set at one-half their width, and r values were set at infinity because no circles could be inscribed. In the case of elongated meristems, the radii were taken directly from circles drawn as the best fit on the apical domes (Fig. 1D) and the width and height were taken as the distance across the meristem at the site of the youngest primordium and the length of the central axis to the width line, respectively. Elongated meristems were assigned θ values of 90°, indicating that the circle was inscribed on their apical domes. Their x/r values were calculated as the sum of $\pi/2$ and y/r, the latter factor representing the additional distance from the circle to the youngest primordium, normalized for the radius. All measurements were incorporated into a Microsoft Excel 97 spreadsheet for performing routine calculations of all variables, for correcting for magnification if needed, and for graphing the relationships among the variables.

All meristem drawings representing different species with alternate, opposite, and whorled phyllotaxes were analyzed to generate model values. For most meristems, the minimal phase occurred just after the initiation of the youngest primordium and the maximal phase occurred just prior to the initiation of the next primordium (for discussion, see Esau, 1965). Meristem measurements were plotted as minimal phase (lowest θ or x/r value) and maximal phase (highest θ or x/r value) for each species.

Chapter 3: Results

Taxonomic distribution of aquatic plant phyllotaxes

Several common aquatic plants do indeed exhibit whorled phyllotaxis, as illustrated by *Ceratophyllum demersum* with an average of six leaves per node, *Hydrilla* sp. with four leaves per node, and *Myriophyllum spicatum* with three or four leaves per node. It was not known, however, if whorled phyllotaxis actually occurs at a greater frequency in aquatic plants as compared to terrestrial plants. Therefore, the Delta angiosperm database including 583 families was screened for any family with at least one hydrophyte species, defined as those plants having vegetative parts submersed in water, floating on water, or partially emergent from water under normal conditions. A preliminary list of 52 hydrophyte families was produced from this database. Further analysis eliminated nine large families composed of over 100 genera from the hydrophyte list, including Acanthaceae, Araceae, Compositae, Cruciferae, Cyperaceae, Graminaceae, Melastomataceae, Rubiaceae, and Scrophulariaceae. These nine families contained a limited number of aquatic members but were more accurately represented as nonhydrophyte families because of a much higher percentage of terrestrial species. Of the remaining 43 families, Crassulaceae, Oxalidaceae, and Ranunculaceae were eliminated from the hydrophyte list because less than 10% of their genera contained aquatic members. Although a few families remaining on the hydrophyte list were composed of a single genus, these families had more than 10% aquatic species and were not eliminated.

After all adjustments, the final subset of hydrophytes consisted of 40 families or 7% of angiosperm families (Table 3).

Additional screens were used to identify the percentage of the three arrangements of mature leaves (alternate, opposite, and whorled) that appeared among angiosperm families as a whole and hydrophyte and nonhydrophyte as subsets. Because of multiple leaf insertion codes per family, the summation of the three phyllotactic screens totaled more than 100%. Irrespective of ecological type, alternate phyllotaxis was the dominant leaf arrangement in 80% of hydrophyte families, 82% of nonhydrophyte families, and 81% across all families (Table 3). Opposite phyllotaxis represented 35% of both hydrophyte and nonhydrophyte families. The most striking difference between hydrophytes and nonhydrophytes appeared in the whorled category. In particular, 38% of hydrophyte families exhibited whorled phyllotaxis, whereas only 15% of nonhydrophyte families had whorled species, thus affirming my initial observation that aquatic plants express whorled phyllotaxis more often than do terrestrial plants.

The whorled, alternate, and opposite groups generated from the database of flowering plant families were also examined for patterns that would prove informative as to the factors potentially involved in different phyllotaxes. Interestingly, the monocots had very few species with opposite phyllotaxis, but these species were almost exclusively classified as hydrophytes. By contrast, the large number of dicot opposites were sorted into both hydrophyte and nonhydrophyte categories (data not shown).

Table 3. Distribution of different phyllotaxes in hydrophyte and non-hydrophyte families in the angiosperms.

Ecological Type	Families		Whorled		Alternate		Opposite	
	Number	%	Number	%	Number	%	Number	%
Hydrophytes	40	7	15	38	32	80	14	35
Non-hydrophytes	543	93	80	15	443	82	188	35
All families	583	100	95	16	475	81	202	35

Geometric analysis of aquatic plant meristems

Ideally, morphological models should be constructed so that the model parameters can be directly related to fundamental structural properties. The traditional rectilinear coordinates of height and width measurements were converted to polar coordinates because height and width, independent of each other, cannot be related to a specific meristem property, such as size, shape, or primordium position. In the model presented here, the displacement angle (θ), or its normalized linear equivalent (x/r), represents an independent measure of primordial position (Fig. 1). The meristem can be divided into two distinct regions consisting of the apical dome shaped like a hemisphere or hemispherical sector and the subtending axis shaped like a regular cylinder or truncated cone. The dividing line between these two regions corresponds to a θ value of 90°, also expressed as 1.57 in linear terms. Hence, lower θ or x/r values correspond to a primordial position close to the dome summit, and higher θ or x/r values correspond to a position away from the summit on the subtending axis beneath the dome. The radius is inversely related to the curvature of the apical dome: a broad meristem with slight curvature is characterized by a high r value, whereas a narrow meristem with pronounced curvature is characterized by a low r value.

Given the cyclical changes in meristem size during primordium initiation, Figs. 2A, 3A, and 4A present minimal and maximal phase data for each species. Particular attention was given to θ and corresponding x/r values associated with the maximal phase, which represented the shoot apex just prior to the emergence of the new primordium. The switch between primordial initiation on the apical dome to the subtending axis was

indicated by a solid line on each graph at $\theta = 90°$ (or $x/r = 1.57$). To reduce the labels needed to identify the points on the graphs, data for associated minimal and maximal phases were connected with a dotted line in Figs. 2A–4A.

The heights and widths of the apical meristems presented in Figs. 2A, 3A, and 4A are illustrated in Figs. 2B, 3B, and 4B. For a given species, the height and width coordinates for the minimal and maximal phases were connected by a solid line (hereafter referred to as the min-max line). The slope of this line represented the ratio of axial growth to lateral growth throughout the plastochron. Thus, those meristems emphasizing axial growth displayed negative slopes or positive slopes greater than one, while other meristems undergoing lateral growth had positive slopes less than one.

Alternate Phyllotaxis

The geometrical characteristics of the shoot apical meristems of two lycophytes (*Isoetes engelmannii* and *I. riparia*), two monocotyledons (*Oryza sativa* and *Potamogeton perfoliatus*), and two dicotyledons (*Proserpinaca palustris* and *Ranunculus flabellaris*) that display alternate phyllotaxis of mature leaves were graphed in Fig. 2. For example, the shoot apex of *Potamogeton perfoliatus* was characterized by a radius of 50 µm and a displacement angle of 32° at the minimal phase and by a radius of 37 µm and an angle of 79° at the maximal phase (Fig. 2A). In general, the meristems of all species except *O. sativa* remained grouped together. These meristems had radii ranging between 36 µm and 74 µm and displacement angles between 32° and 79° at their maximal phases, signifying that the youngest primordial on these meristems were initiated on the apical dome itself.

Fig. 2 Geometrical measurements characterizing minimal and maximal phases of apical meristems of aquatic plants with alternate phyllotaxis. (A) Linear and angular displacement values characteristic of minimum (open circles) and maximum (closed circles) phase meristems. For each species, the samples with the smallest and largest normalized linear displacement were taken to represent the minimal and maximal phases respectively. Data points for the phases of each species are connected with a dotted line. (B) Height and width measurements that correspond to the minimum and maximum phases in A. Data points for the phases of each species are connected with a solid line. *h*, height; *r*, radius; *w*, width; *x/r*, normalized linear displacement; θ, angular displacement.

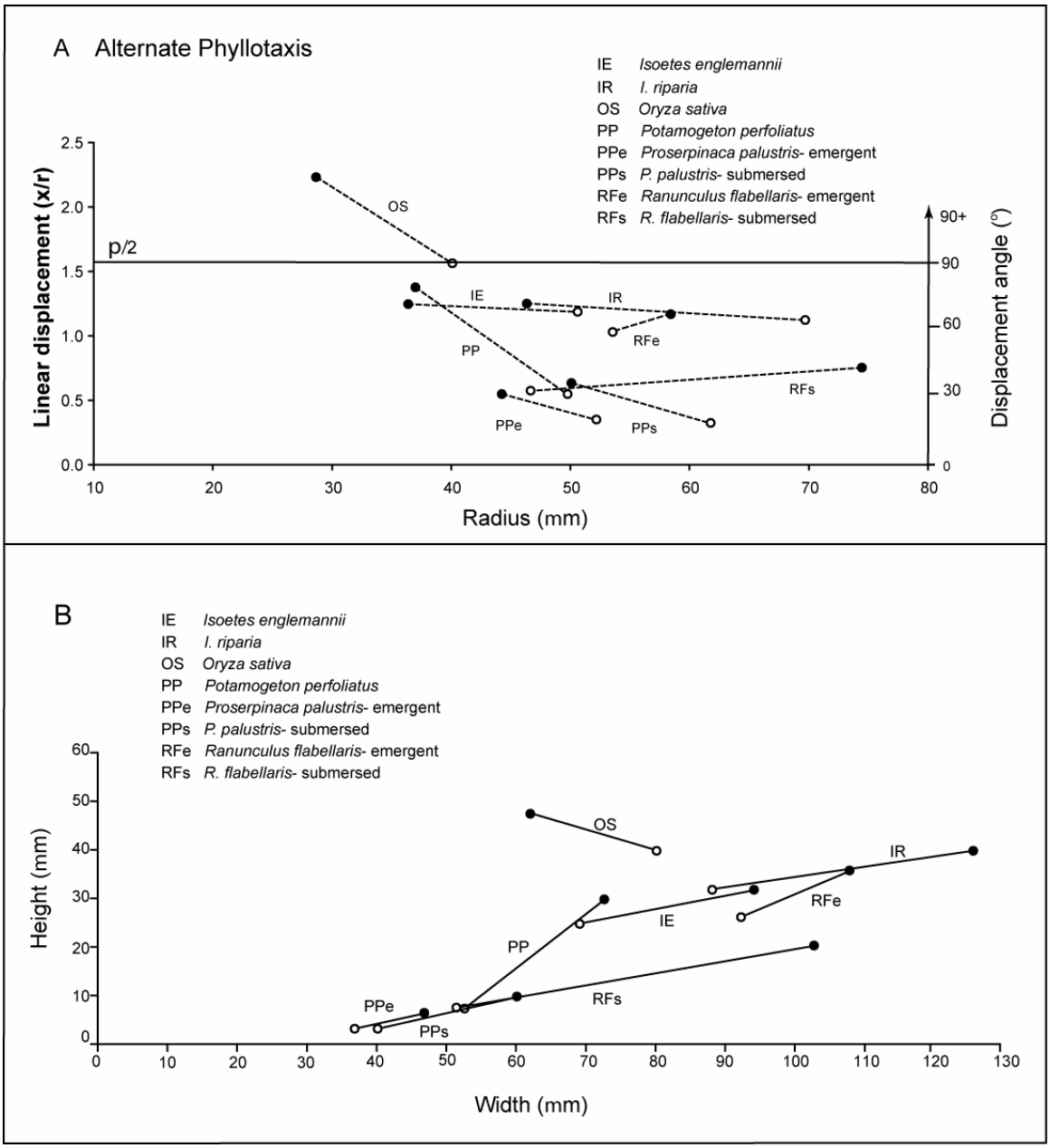

The meristem of *O. sativa*, with a slightly smaller radius of 29 μm, had displacement angles equal to or greater than 90° in both phases and corresponding *x*/*r* values of 1.57 at minimal phase and 2.24 at maximal phase. Thus, the youngest primordium on this meristem developed on the axis subtending the apical dome. Interestingly, unlike other primordia in this category, this primordium rapidly encircles the apical meristem soon after its inception (Sharman, 1945).

Height and width measurements were also taken for the same group of alternate species and graphed in Fig. 2B. A min-max line was drawn to indicate the growth dynamics during the plastochron. The shoot apical meristem of *Potamogeton perfoliatus*, my earlier example, had a height and width of 8 μm and 53 μm, respectively, during the minimal phase and 30 μm and 73 μm, respectively, at its maximal phase. The dimensions of the minimal phases of alternate meristems ranged from 3 μm to 32 μm in height and from 37 μm to 92 μm in width, and their maximal phases ranged from 7 μm to 40 μm in height and from 47 μm to 126 μm in width. The meristems of *Oryza sativa* exhibited an exceptional height of 48 μm at maximal phase. As indicated by the positive slope of the min-max lines, the meristems of all species except *O. sativa* increased in both height and width during the plastochron. In addition, the majority of the slopes appeared relatively flat, signifying that their plastochronic dynamics emphasized lateral as opposed to axial growth. The min-max line for *Potamogeton perfoliatus* had a slope of 1.13, which indicated that this meristem experiences roughly equal growth in both directions. The negative slope for the meristematic growth of *O. sativa* revealed that this meristem underwent axial growth at the expense of lateral growth.

Because *Ranunculus flabellaris* and *Proserpinaca palustris* meristems can be found above or below the water's surface, geometrical measurements were taken from both emergent and submersed meristems to evaluate the effect of environmental conditions on meristem geometry. In both species, the maximal phase of the emergent meristem had a smaller *r* value, which corresponded to a less protuberant shape. The displacement angles of maximal phase of the emergent and submersed *P. palustris* meristems were almost identical. A greater difference was observed in *R. flabellaris* where the emergent displacement was greater than that in the submersed form (Fig. 2A). In both species, the overall geometry of these meristems fell within the typical range for alternate plants. The displacement angles did not exceed 90°, indicating that the primordia were initiated on the meristem dome. Although the emergent meristems of both heterophyllic species had steeper min-max lines than the corresponding submersed meristems, these slopes remained below a value of one (Fig. 2B). Thus, the plastochron dynamics of these meristems were not significantly affected by their position relative to the water's surface.

Opposite Phyllotaxis

The dimensions of radius (*r*), angular displacement (θ), and its linear counterpart (*x*/*r*) were collected from 10 species including three monocotyledons (*Najas guadalupensis*, another *Najas* sp., and *Zannachellia palustris*) and seven dicotyledons (*Callitriche heterophylla*, *Cabomba* sp., *Dianthera americana*, *Ludwigia pervensus*, *Bacopa monnieria*, *Bacopa carolinia*, and *Rotalia indica*) that display opposite phyllotaxis of mature leaves (Fig. 3A). Typical of the shoot apical meristems of most dicotyledons, *D. Americana* was characterized by an *r* value of 82 μm and a θ value of 25° during its

minimal phase. At the maximal phase of the plastochron, its *r* value d decreased to 52 μm and θ value increased to 59°. The meristems of all dicotyledons except *Callitriche heterophylla* had radii in the range of 40–77 μm and θ in the range of 39°–77° during the maximal phase. Thus, these meristems initiated new primordia on their apical domes. The four remaining species, the dicotyledon *Callitriche heterophylla* (including both the emergent [CHe] and submersed [CHs] specimens), and the monocotyledons *N. guadalupensis* (NG), *Najas* sp. (NS), and *Z. palustris* had apical meristems whose θ values were ≥ 90° and *x*/*r* values of 1.57 (CHe), 1.96 (CHs), 2.47 (NG), and 2.92 (NS) at their maximal phases. Therefore, these meristems initiated new primordia on the subtending axis below the apical dome.

The min-max lines, representing the plastochronic changes in meristems for opposite plants, are seen in Fig. 3B. Again, using *Dianthera americana* as a typical opposite plant, the minimal phase of its meristem was 8 μm in height and 69 μm in width, and the maximal phase was 26 μm in height and 89 μm in width. As a group, the apical meristems of dicot opposite species had ranges of 2–50 μm in height and 42–72 μm in width during the minimal phases and 17–32 μm in height and 48–89 μm in width during the maximal phases. The monocotyledons *Najas* sp. (NS), *N. guadalupensis* (NG), and *Z. palustris* had the greatest heights within this group, but they exhibited average widths. Conversely, the meristems of the dicotyledon *Cabomba* sp. had widths outside those seen for other opposites, 108 μm at minimum and 97 μm at maximum, but maintained heights typical of other meristems of plants developing opposite phyllotaxis. The meristems of all dicotyledons excluding *Cabomba* sp. had min-max lines with positive slopes. Four

meristems displayed min-max lines with slopes less than one, indicating that their plastochronic dynamics emphasized lateral and not axial growth. Two meristems had slopes greater than one, representing a greater emphasis on axial growth. The remaining species, including all three monocotyledons plus the dicotyledon *Cabomba* sp., produced min-max lines with negative slopes, which illustrated a pronounced emphasis on axial growth during their plastochrons.

Included among the opposite plants was one heterophyllic species, *Callitriche heterophylla*. A comparison of the emergent vs. submersed meristems revealed that during the maximal phase, the emergent meristem had a slightly larger radius, 24 µm vs. 19 µm, and a smaller linear displacement (x/r), 1.57 vs. 1.96 (Fig. 3A). However, based on the displacement values of both these meristems, primordia were initiated on the subtending axis beneath the apical dome. Even smaller differences were seen in the height and width measurements of submersed vs. emergent apices (Fig. 3B). The steep slopes of both min-max lines reflected the predominance of axial growth during their plastochrons.

Whorled Phyllotaxis

The normalized linear and angular displacements were plotted against dome curvature for eight whorled species including two monocotyledons, *Anacharis densa* (5 *Elodea densa*) and *Hydrilla* sp., and six dicotyledons, *Ceratophyllum densa*, *Hippuris vulgaris*, *Myriophyllum heterophyllum*, *M. spicatum*, *M. aquaticum*, and *Rotalia indica* (Fig. 4A). *Anacharis densa*, commonly used in text as an example of whorled phyllotaxis, had a meristematic radius of 42 µm during its minimal phase and 44 µm during its maximal

Fig. 3. Geometrical measurements characterizing minimal and maximal phases of apical meristems of aquatic plants with opposite phyllotaxis. (A) Linear and angular displacement values characteristic of minimum (open circles) and maximum (closed circles) phase meristems. For each species, the samples with the smallest and largest normalized linear displacement were taken to represent the minimal and maximal phases respectively. Data points for the phases of each species are connected with a dotted line. (B) Height and width measurements that correspond to the minimum and maximum phases in A. Data points for the phases of each species are connected with a solid line.

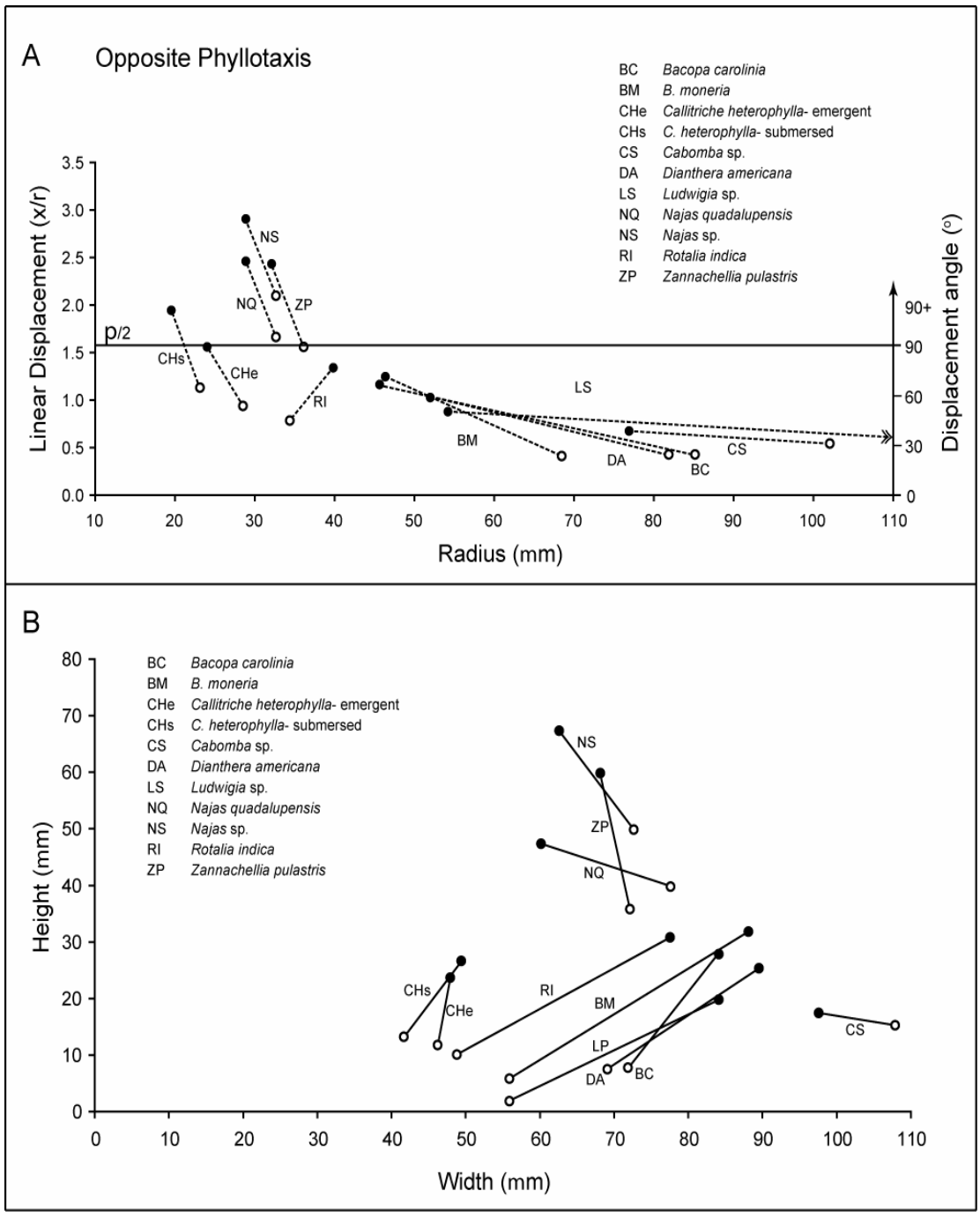

Fig. 4. Geometrical measurements characterizing minimal and maximal phases of apical meristems of aquatic plants with whorled phyllotaxis. (A) Linear and angular displacement values characteristic of minimum (open circles) and maximum (closed circles) phase meristems. For each species, the samples with the smallest and largest normalized linear displacement were taken to represent the minimal and maximal phases respectively. Data points for the phases of each species are connected with a dotted line. (B) Height and width measurements that correspond to the minimum and maximum phases in A. Data points for the phases of each species are connected with a solid line.

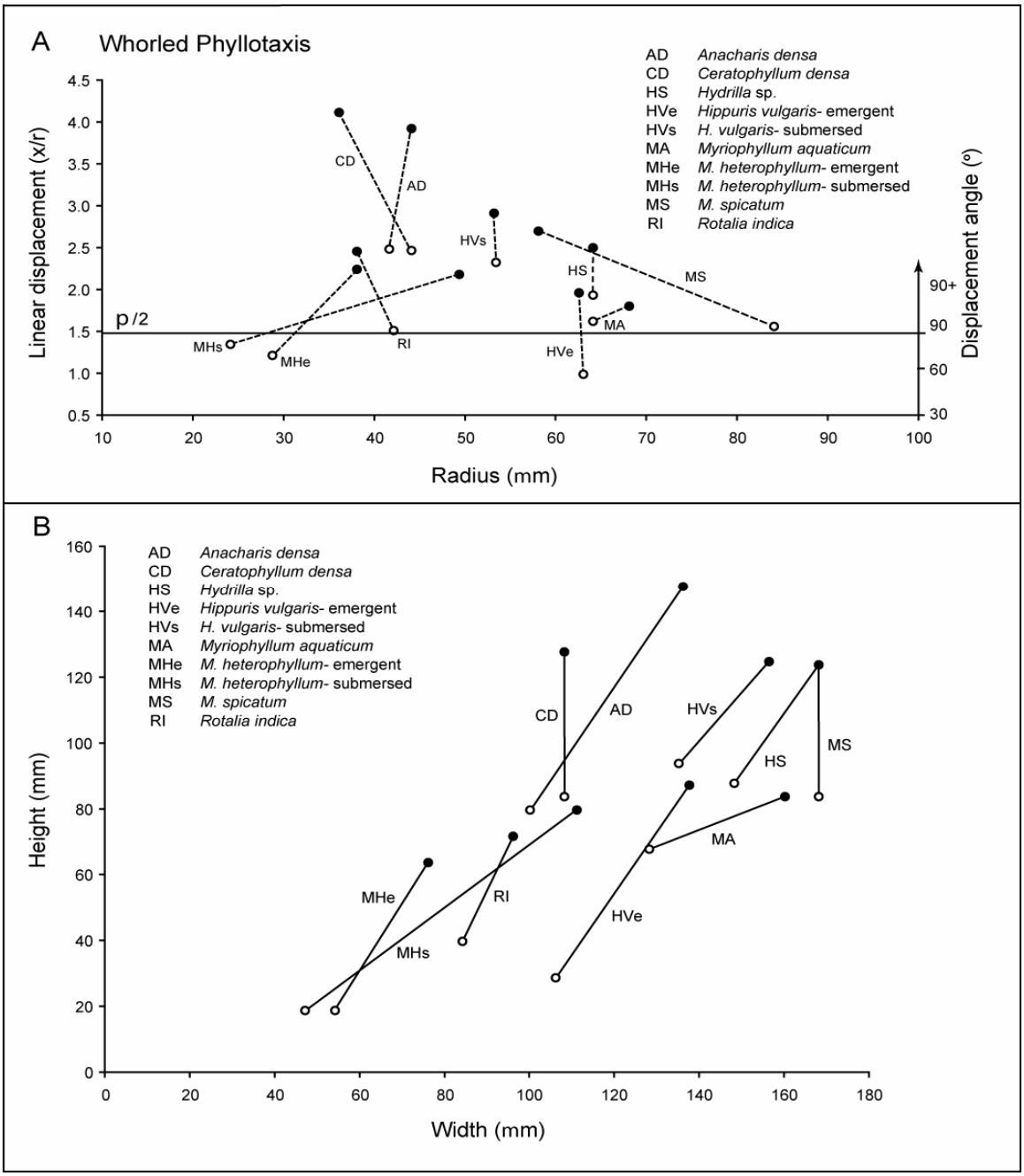

phase, which indicated that the curvature of its apical dome remains constant over the plastochron. In both phases, angular displacement (θ) was greater than 90° as evidenced by a minimal normalized linear displacement of 2.5 and a maximal linear displacement of 3.9. The eight whorled species sampled had a wide range of meristematic radii with maximal phases between 36 µmm and 68 µm, and normalized linear displacements between 1.8 and 4.1. These data show that, without exception, all whorled species in this study initiated primordial on the axis subtending the apical dome.

During the plastochron, *Anacharis densa* had a height of 80 µm and width of 100 µm at minimal phase and a height of 148 µm and a width of 136 µm at maximal (Fig. 4B). Overall, the apical meristems of whorled species ranged from 19 µm to 94 µm in height and 47 µm to 168 µm for width during the minimal phase. Every meristem in this group increased in height and width during the plastochron with maximal phases that ranged from 64 µm to 148 µm for height and 76 µm and 168 µm for width. As a result, almost all min-max lines had positive slopes; therefore, these species emphasized axial growth. Exceptions included *Myriophyllum heterophyllum* (submersed) and *M. aquaticum* meristems, which had slopes close to one, corresponding to a balance between axial vs. lateral growth.

Whorled submersed and emergent meristems were observed in the cases of *Myriophyllum heterophyllum* and *Hippuris vulgaris*. Submersed meristems of *Hippuris vulgaris* had greater displacement angles and heights than emergent meristems, while all

Myriophyllum heterophyllum meristems tended to have overlapping ranges. Both species were similar to other whorled plants in that primordia were initiated on the subtending axis of the apical dome. In addition, both species experienced plastochron growth dynamics similar to the other whorled plants.

Overall Comparisons

The radii of the apical domes of aquatic plants fell within an overlapping range from 36 µm to 77 µm at the maximal phase. Thus, apical curvature had no apparent influence on the phyllotactic pattern chosen. By contrast, maximal phase displacement angles equal to or greater than 90° were exclusive to whorled species. Therefore, a large displacement from the dome, which resulted in the initiation of primordia on the subtending axis of the dome, was a necessary characteristic of whorled phyllotaxis. With the exception of one alternate (*Oryza sativa*) and several opposite species (*Callitriche heterophylla*, *Najas guadalupensis*, *Najas* sp., and *Zannachellia palustris*), all meristems with either alternate or opposite phyllotaxis exhibited smaller displacement angles associated with primordial initiation on the apical dome. Similarly, the growth dynamics in the meristems of whorled plants and those exceptional plants listed before had pronounced axial growth at the expense of lateral growth, which differed from the greater emphasis on lateral growth in all other alternate and many opposite plants.

Heterophyllic species were present in all three categories of phyllotactic patterns. In general, the submersed meristems of heterophyllic species were characterized by greater heights and greater normalized linear displacements at the maximal phase than comparable emergent meristems with the result that the submersed meristems extended

farther above the existing leaf primordia. However, no differences in the phyllotactic patterns originating from submersed vs. emergent meristems were observed in the heterophyllic species examined in this study.

Chapter 4: Discussion and Conclusions

Geometric relationships underlying phyllotactic patterns

This thesis is predicated on the notion that the phyllotactic patterns of leaf primordia may depend on a simple relationship between meristem geometry and primordial position. Thus, the rectilinear parameters of height and width that are conventionally used as quantitative measures of apical geometry were transformed into the polar coordinates of radius (*r*) and displacement angle (θ) that are directly related to meristem curvature and primordial position, respectively. The resulting data in Figs. 2A, 3A, and 4A establish that the primordia arranged in alternate and opposite phyllotaxis tend to have low θ values at maximal phase, i.e., they arise high on the apical dome, while primordia arranged in whorled phyllotaxis tend to have θ values >90° at maximal phase, i.e., they arise off the apical dome on the subtending axis.

I propose that these observations disclose several fundamental geometrical relationships that represent ground states for phyllotactic patterning. Typically, the apical dome bears its primordia in alternate arrangements that are usually characterized as two spirals radiating across the dome. On the other hand, the subtending axis bears its primordia in whorled arrangements that consist of successive rings of several primordia wrapped around the axis. Therefore, it seems reasonable to conclude that these observations reveal the primary geometrical principle relating apical geometry to primordial phyllotaxis: (A) *primordia arising on the apical dome tend to assume a spiral arrangement,* and (B)

primordia arising on the subtending axis tend to assume a whorled arrangement (Fig. 5). In the latter case, the primordia of whorled species can initially arise on the axis as a unified ring, which will then differentiate into separate primordia (*Equisetum* and *Ceratophyllum*: Rutishauser and Sattler, 1987), or they can arise as discrete primordia positioned in an whorled arrangement (*Anacharis*: Clowes, 1961).

The literature has not explicitly recognized this primary relationship between primordial position and phyllotactic arrangement mentioned before. On the other hand, the literature has repeatedly mentioned the secondary geometrical principle relating primordial size to available space: (A) *the smaller the primordial size relative to overall dome size, the higher the Fibonacci or auxiliary numbers needed to characterize that spiral arrangement* (Williams, 1975: Fig. 3.8; Jean, 1994; Lyndon, 1998), and (B) *the smaller the primordial size relative to the overall annulus (or ring) size, the greater the number of primordia arising in the resulting whorl* (Fig. 5.). In the latter case, the aquatic *Hippuris vulgaris* has an elongated meristem with several primordial rings forming on the

Fig 5. Diagrammatic summary of the geometric relationships governing phyllotaxis. The primary principle relates the sites of primordial initiation to the overall phyllotaxis, i.e. primordia arising on the apical dome are often positioned in spiral arrangements, while primordia arising on the subtending axis are arranged in whorled patterns. The second principle relates the ratio of primordial size to available space to quantitative features of the overall phyllotaxis. Different spiral phyllotaxes are illustrated by the apical meristems of *Brassica oleracea*, *Linum usitatissimum*, *Helianthus annuuss*, which show that the ratio of the size of young primordia to the apical dome is inversely correlated with the magnitude of the Fibonacci numbers charactering these phyllotaxes. Reproduced with permission from Williams, (1975). Different whorled phyllotaxes are illustrated by the apical meristems of rice, *Najas* and *Anacharis* which show that the ratio of the size of young primordia to the axis annulus is inversely correlated with primordial number in these phyllotaxes.

1st Geometric Principle

2nd Geometric Principle

Primordia arise on the dome

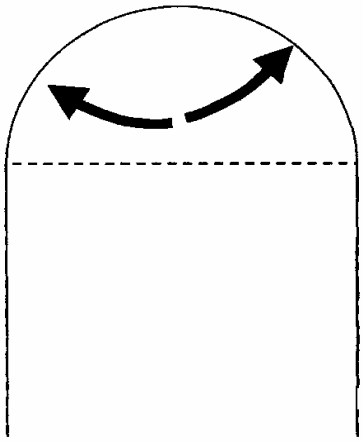

Spiral Phyllotaxis

Examples:

Brassica oleracea

Linum usitatissimum

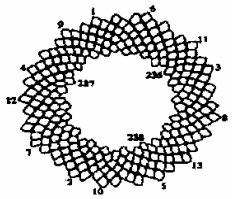

Helianthus annuus

Phyllotactic Ratio

1/2

3/5

34/55

Primordium size / Apical dome size

High

Low

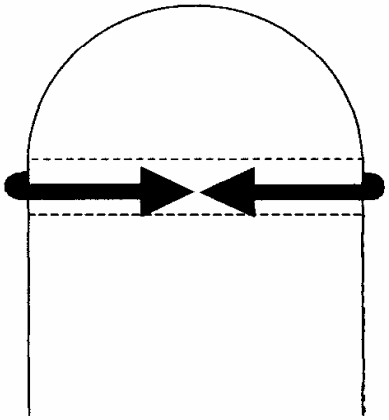

Annular Phyllotaxis

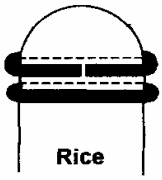

Rice

Najas

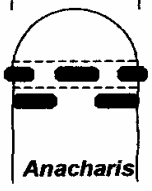

Anacharis

Primordia/ Annulus

1

2

4

Primordium size / Annulus diameter

High

Low

subtending axis below the apical dome; an increase in primordial number in each whorl is directly correlated with an increase in annulus diameter (McCully and Dale, 1961). Several whorled terrestrial species, including *Equisetum arvense* (Bierhorst, 1959), *Ephedra altissima* (Gifford, 1943), and *Casuarina distyla* (Williams and Metcalf, 1985), have this same correlation (Fig. 6).

One compelling feature of the geometrical model depicted in Fig. 5 is its ability to account for exceptional observations. For example, the apical meristem of domesticated rice, *Oryza sativa*, is unique among my sample of aquatic species with alternate phyllotaxis because its primordia are initiated on the subtending axis below an elongated meristem (Fig. 2A). Therefore, the apical meristems of rice plants have the same geometric features as the meristems of typical whorled species except that rice, like the

Fig. 6. Apical meristems of terrestrial plants exhibiting annular phyllotactic patterns. (A) Median longitudinal section of the shoot apex of *Equisetum arvense*, with whorled phyllotaxis. Reproduced with permission from Kaplan (2001). (B) Median longitudinal section of shoot apex of *Ephedra altissima* with whorled phyllotaxis. Reproduced with permission from Paolillo and Gifford, (1961). (C) Three-dimensional reconstruction of the shoot apex of *Casuarina distyla*, with whorled phyllotaxis. Reproduced with permission from the *Australian Journal of Botany* (Williams and Metcalf, 1985) with permission of CSIRO Publishing. (D) A vegetative stem apex of *Secale cereale*, with whorled phyllotaxis consisting of single encircling primordium in each whorl. Reproduced with permission from Koller et al., (1960). (E) Scanning electron migcrograph of the shoot apex of *Galium rubioides*, which is best interpretedas a whorl-mimic composed of two leaf primordia and several leaflike stipules. Reproduced with permission from Rutishauser (1984). (F) Three-dimensional reconstruction of the shoot apex of *Nerium oleander* exhibiting the transition from decussate to tricussate phyllotaxis. The primordia labeled L8 consist of one larger primordium and a second primordium bisected into two smaller adjacent primordia, which is then followed by a whorl of three equidistant and equal-sized primordia, labeled L9. Reproduced with permission from *Australian Journal of Botany* (Williams et al. 1982) with permission of CSIRO Publishing.

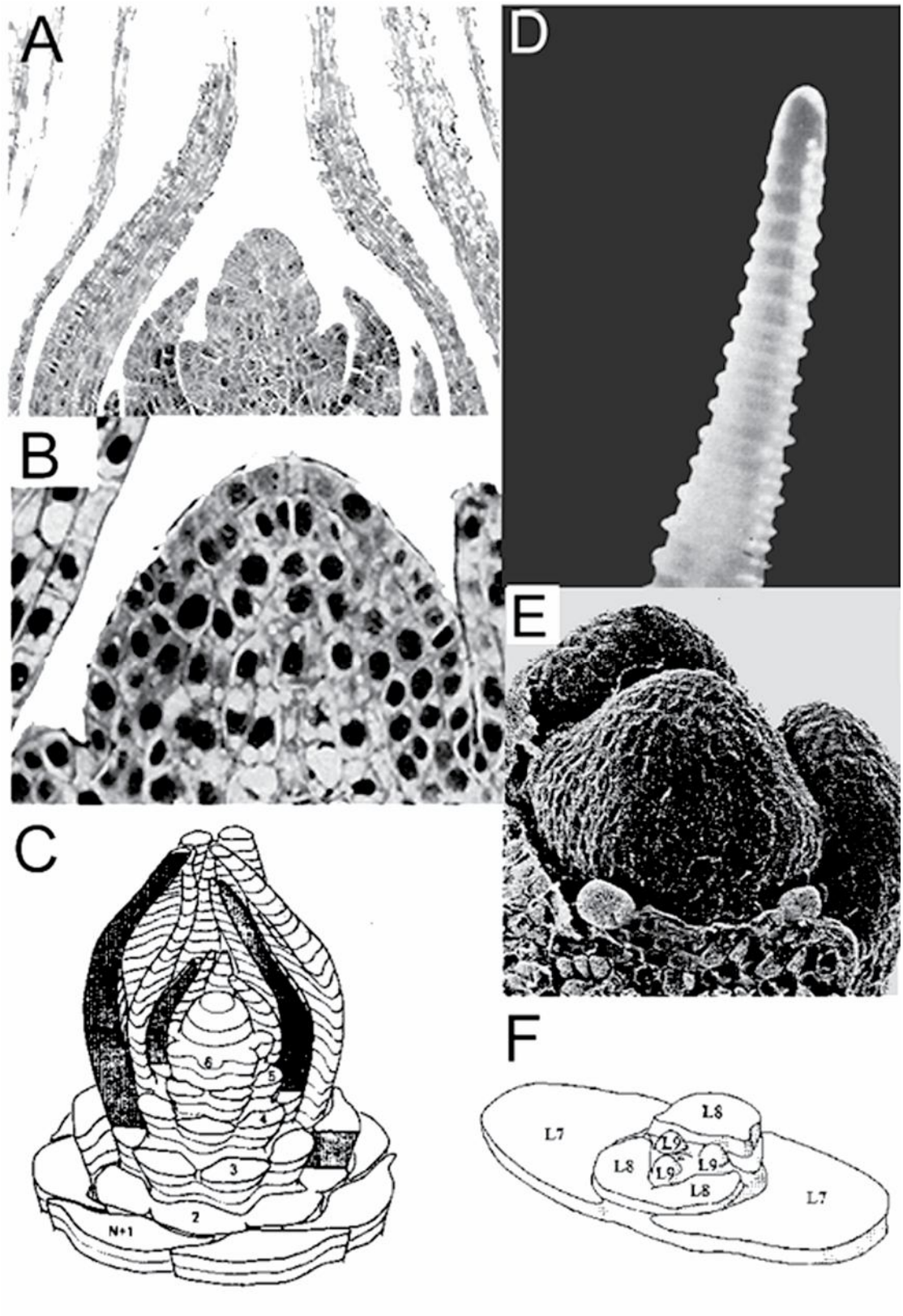
A
B
C
D
E
F
6
5
4
3
2
N+1
L7
L8
L9
L8
L9
L9
L8
L7

other grasses (Fig. 6D), develop single clasping primordia that encircle the entire axis (Fig. 5) in place of smaller multiple primordia. Thus, the alternate phyllotaxis of the rice plant is more appropriately interpreted as a whorl of one primordium as opposed to a type of spiral phyllotaxis.

This interpretation is strongly supported by morphological evidence from the apical meristems of grass mutants. My geometrical model predicts that a change in the site of primordial initiation from the axis to the dome should result in the corresponding switch from whorled to spiral phyllotaxis. In particular, the rice *sho* mutants are characterized by flatter meristems, young primordia on the apical dome, and nonclasping leaves. It is entirely consistent with my model that *sho* mutants have an irregular spiral phyllotaxis with horizontal divergence angles approaching the 138° angle characteristic of Fibonacci based patterns (Itoh et al., 2000). Furthermore, it follows from the geometrical model that a decrease in the ratio of primordial size relative to annulus diameter should result in more than one primordium being initiated in the annulus. In wild-type maize, the primordium encircles the meristem to such an extent that the margins of the primordium overlap each other. By contrast, the maize mutant *abphyl* exhibits a profound increase in meristem size without a compensatory increase in primordial size. As a result, the axis can accommodate the simultaneous initiation of two primordia in an opposite arrangement (Greyson et al., 1978: cf. Fig. 1 vs. Fig. 4). In conclusion, these mutants confirm the fundamental validity of applying the ‘‘whorl of one’’ concept to grass phyllotaxis.

The opposite monocots also offer an intriguing opportunity to evaluate my model. In principle, opposite phyllotaxis can be viewed as a special case of whorled phyllotaxis consisting of two primordia that arise at the same level. Because monocot embryos develop a single cotyledon, all monocots must initially express alternate phyllotaxis by default. Thus, opposite monocots have subsequently switched from alternate to whorled phyllotaxis. Interestingly, the limited number of monocot families that are reported as typically having opposite phyllotaxis is almost exclusively composed of aquatic species (Dallwitz et al., 2000; Watson and Dallwitz, 2000). It is noteworthy that all aquatic opposite monocots in Fig. 3 initiate their primordia on elongated, narrow apices, with displacement angles greater than 90°, thus corresponding to the same location for primordial initiation in all aquatic whorled species (Fig. 4A). Thus, it follows as a reasonable conclusion that these monocots switched to a whorled phyllotaxis of two primordial once the leaves arose off the apical dome in an annulus large enough to fit two primordia (Fig. 5).

In marked contrast to the restricted occurrence of opposite phyllotaxis in monocot families, this phyllotactic pattern is widespread among dicot families. Almost all dicots produce two cotyledons that arise in an opposite arrangement near the apex of the globular embryo (Gifford and Foster, 1989; Kaplan and Cooke, 1997). That these opposite patterns are initiated on the apical domes of dicot embryos implies that these embryos are not constrained by the same geometrical relationships observed on other whorled species. Thus, dicot embryos are apparently able to override the basic geometrical relationships to produce the equivalent of an opposite phyllotaxis on their

apical dome. This opposite arrangement of dicot cotyledons is converted to postembryonic arrangements of different spiral phyllotaxes in up to 85% of dicot seedlings (Meicenheimer, 1998), which is consistent with the new leaves being initiated on the apical dome. However, the other 15% of dicot species remain locked into the embryonic pattern of opposite cotyledons that becomes their postembryonic pattern of leaf phyllotaxis. Despite their primordia having displacement angles >90°, most opposite aquatic dicots measured in Fig. 3 have this mode of persistent opposite phyllotaxis. By contrast, the apical meristems of *Callitriche heterophylla* produce new primordia with displacement angles around 90°, which may be indicative of a genuine whorled phyllotaxis composed of two small primordia arising on the subtending axis. Lastly, several dicot families develop monocotyledonous embryos (for references, see Gifford and Foster, 1989), and the phyllotactic arrangements of these plants, as would be expected from geometric principles, are invariably spiral.

In summary, the analysis of meristem geometry of aquatic plants depicted in Figs. 2–4 leads to the realization that their apices produce new primordia in two fundamental patterns: (1) spiral patterns, which are produced by new primordia arising at different levels on the apical dome, and (2) whorled patterns, which result from one or more primordia arising in a complete ring around the subtending axis. These geometrical relationships are validated by their ability to account for the unexpected axial positions of new primordia in the instances of the alternate phyllotaxis of rice plants and the opposite phyllotaxis of aquatic monocots. However, these relationships are frequently overridden

by unknown biological mechanisms in the case of most dicots that have persistent opposite phyllotaxis.

Evolution of whorled phyllotaxis in aquatic plants

The aquatic species examined in this thesis have almost exclusively generated whorled phyllotaxis via the formation of lateral primordial on an elongated meristem. Thus, the repeated evolution of whorled phyllotaxis in aquatic plants (see introduction) appears to depend in part on the potential of elongated meristems to evolve in aquatic environments. Two observations hint at potential selection pressures operating on meristem shape itself. Firstly, the height of emergent meristems of all heterophyllic species, excluding *Ranunculus flabellaris*, was significantly reduced relative to submersed meristems (Figs. 2–4B). Conversely, xeric plants like cacti often possess flat or sunken meristems that are embedded underneath the surrounding subapical structures (Boke, 1951, 1954, 1955). Thus, aquatic environments seem to be more permissive toward exposed meristems in contrast to terrestrial environments where the desiccating effects of even intermittent exposure appear to select for more protected meristems.

The relative amount of light harvesting is a second potential selection pressure operating on phyllotactic pattern. In computer simulations, light harvesting is maximized by whorled phyllotaxis provided that the leaves within each whorl do not overlap and the internodal distance equals or exceeds leaf length (Niklas, 1998). Thus, it could be argued that whorled phyllotaxis may be favored in both submerged aquatic and shaded terrestrial environments where light penetration is often limiting (for compensate ing factors, see Niklas, 1998). Because most terrestrial plants lack the elongated meristems characteristic

of aquatic plants with whorled phyllotaxis, then the question becomes, How do certain terrestrial plants develop equivalent types of this phyllotactic pattern?

Exceptional examples of whorled phyllotaxis in terrestrial plants

It is critical to confirm that the fundamental geometrical relationships underlying phyllotactic arrangements described for aquatic plants are applicable to all plants. My initial survey of the meristem geometry of terrestrial plants (data not shown) indicated that they do generally follow the fundamental geometric relationships illustrated in Fig. 5. In particular, a few terrestrial plants, such as *Equisetum arvense*, *Ephedra altissima*, and *Casuarina distyla*, produce elongated meristems with multiple primordia arising in each whorl on the subtending axis (Fig. 6A–C). However, the less protuberant, compressed meristems of most other terrestrial plants appear to be geometrically restricted from generating whorled arrangements of young primordia. Then it comes as no surprise that terrestrial plants tend to favor spiral arrangements of their primordia, with the exception of the 15% of dicots locked in an embryonic opposite pattern, as described earlier.

Terrestrial plants have, nevertheless, adopted several different developmental mechanisms for altering the primordial phyllotaxis into either whorl-mimics or pseudowhorls. One example of a nongeometrical mechanism for creating whorlmimics involves the modification of stipules into leaflike organs. For example, the dicot *Galium rubioides* (Fig. 6E) produces a whorl of leaflike structures that consists of two leaves and 4–6 stipules that are transformed into leaflike organs (Takeda, 1916; Troll, 1943). Although Rutishauser (1984) argues that these modified stipules are genuine foliage

leaves, the weight of morphological evidence, such as the absence of associated buds, discloses their stipular nature. Thus, I interpret the whorl-mimicking phyllotaxis of this genus as originating from the interaction of two nongeometric factors: the basic pattern of a locked opposite arrangement resulting from the persistent embryonic condition, which is subsequently modified through enhanced stipular growth.

A second nongeometrical mechanism appears to involve the separation of a single primordium into two primordia. For example, the dicot *Nerium oleander* exhibits an opposite (i.e., decussate) phyllotaxis during early vegetative growth. Because *N. oleander* develops a flat meristem (Williams et al., 1982), this postembryonic pattern must also be attributed to the persistence of embryonic patterning. However, the higher nodes of this plant have an intriguing transitional state between the original decussate and the later tricussate phyllotaxes (Fig. 6F; Williams et al., 1982). This transitional state has one large primordium (L8, upper right) opposite two adjacent small primordial (L8, lower left), which is reasonably interpreted as representing the other large primordium being congenitally split into two primordia. In higher whorls (L9), the transitional state is obscured as the smaller primordia assume the size of the large primordium and are repositioned at 120° divergence angles around the apex. Another example of this type of whorl-mimic is *Abelia*, which ha s transitions from trimerous to tetramerous whorls (Douady and Couder, 1996c: Fig. 13). Thus, these whorl-mimics are also generated by persistent embryonic patterning and altered primordial growth.

The third common mechanism for creating a whorled appearance in terrestrial plants does not involve the alteration of primordial organs. Instead, the subapical elongation of certain adjacent internodes is altered so that primordia that were initiated at different levels on the meristem are now closely positioned on the mature shoot, thereby creating pseudowhorls (for many examples, see Schoute 1921, 1925, 1936, 1938). In *Peperomia verticillata*, pseudowhorls result from the limited elongation of certain internodes in both spiraled and whorled species (Kwiatkowska, 1999). Those pseudowhorls derived from spiral patterns are more likely to experience a fluctuating leaf number in contrast to those resulting from the combining of two whorled nodes, which are always double the number found in the original whorl. Lastly, while almost all examples of the pseudowhorled arrangement are found on terrestrial plants, each vertical shoot of the marine plant *Halophila engelmannii* bears a single pseudowhorl that is derived from a compressed distichous phyllotaxis (data not shown).

It is clear from this brief survey that phyllotactic patterning in many aquatic plants illustrates the potential for a morphogenetic process to occupy what might be called the biophysical ground state. By contrast, this same process in certain terrestrial plants illustrates the potential for some plants to evolve specific biological mechanisms that override the ground state to achieve another developmental outcome.

General considerations about the mechanistic basis of phyllotactic patterns

The observations reported in this thesis have significant implications for future efforts to construct mechanistic models for phyllotactic patterning. In the past, it has been

universally assumed that the meristem is realistically modeled as a transverse polar projection (for recent examples, see Jean and Barabe´, 1998). In particular, Green (1999) represents the shoot apex as a planar surface bearing concentric, leaf-generating annuli surrounding the apex center. Other workers make explicit statements that meristem geometry need not be considered as an important parameter in their physical models and computer simulations of phyllotactic patterning (e.g., Douady and Couder, 1996a, b). Although these models are generally successful to the extent that they can generate either whorled (e.g., Green et al., 1996; Green, 1999) or spiral patterns (e.g., Mitchison, 1977; Douady and Couder, 1996a, b, c), they have been unable to account for the transitions between these patterns without contrived explanations about optimal packing. My results argue very strongly that the site of primordial initiation specifies the subsequent phyllotactic pattern, which means that pattern transitions can readily be accomplished by subtle alterations in the dynamics of meristematic growth vs. primordial initiation.

My observations indicate that the three types of mature phyllotaxis, alternate, opposite, or whorled, are each generated by several different developmental processes. For instance, whorled phyllotaxis can arise from various processes, including whorled patterns of primordial initiation, altered dynamics of primordial growth, or non-uniform internodal elongation. If the geometrical relationships presented here prove to represent a true ground state that holds for all angiosperms, then future modeling efforts should focus on the simple geometrical relationships specifying phyllotactic pattern as opposed to the more complicated situations in which uncharacterized biological processes override those relationships.

It remains plausible that separate physicochemical mechanisms may be operating to generate either spiral phyllotaxis on the dome or whorled phyllotaxis on the axis. However, the evidence available suggests that a single mechanism interprets meristem geometry in order to produce the appropriate phyllotaxis for each potential site of primordial initiation. Given that many angiosperm lineages have repeatedly re-invaded the aquatic environments, it is striking that no aquatic plants with elongated meristems have retained spiral phyllotaxis, which might be expected in the unlikely circumstance that each whorled aquatic had to evolve its own mechanism de novo for generating that phyllotaxis.

Bibliography

ARBER, A. 1920. Water plants: a study of aquatic angiosperms. University Press, Cambridge, UK.

BIERHORST, D. W. 1959. Symmetry in *Equisetum*. *American Journal of Botany* 46: 170–179.

BOKE, N. H. 1951. Histogenesis of the vegetative shoot in *Echinocereus*. *American Journal of Botany* 38: 23–38.

BOKE, N. H. 1954. Organogenesis of the vegetative shoot in *Pereskia*. *AmericanJournal of Botany* 41: 619–637.

BOKE, N. H. 1955. Development of the vegetative shoot in *Rhysalis cassytha*. *American Journal of Botany* 42: 1–10.

BOSTRACK, J. J., AND W. F. MILLINGTON. 1962. On the determination of leaf form in an aquatic heterophyllous species of *Ranunculus*. *Bulletin of the Torrey Botanical Club* 89: 1–20.

CLARK, S. E., R. W. WILLIAMS, AND E. M. MEYEROWITZ. 1997. The *CLAVATA1* gene encodes a putative receptor kinase that controls shoot and floral meristem size in *Arabidopsis*. *Cell* 89: 575–585.

CLOWES, F. A. L. 1961. Apical meristems. Blackwell Scientific, London, UK.

COOK, C. D. K. 1970. Water plants of the world. Dr. W. Junk, The Hague, Netherlands.

COOK, C. D. K. 1999. The number and kinds of embryo-bearing plants which have become aquatic: a survey. *Perspectives in Plant Ecology, Evolution and Systematics* 2: 79–102.

DALLWITZ, M. J., T. A. PAINE, AND E. J. ZURCHER. 2000. User's guide to Intkey: a program for interactive identification and information retrieval, 1st ed. http://biodiversity.uno.edu/delta.

DESCHAMP, P. A., AND T. J. COOKE. 1985. Leaf dimorphism in the aquatic angiosperm *Callitriche heterophylla*. *American Journal of Botany* 72: 1377–1387.

DODOENS, R. 1578. A Niewe Herball, or Historie of Plantes (English translation by Henry Lyte Esquyer). Gerard Dewes, London, UK.

DOUADY, S., AND Y. COUDER. 1996a. Phyllotaxis as a dynamical self organizing process. Part I: The spiral modes resulting from time-periodic iterations. *Journal of Theoretical Biology* 178: 255–274.

DOUADY, S., AND Y. COUDER. 1996b. Phyllotaxis as a dynamical self organizing process. Part II: The spontaneous formation of periodicity and the coexistence of spiral and whorled patterns. *Journal of Theoretical Biology* 178: 275–294.

DOUADY, S., AND Y. COUDER. 1996c. Phyllotaxis as a dynamical self organizing process. Part III: The simulation of the transient regimes of ontogeny. *Journal of Theoretical Biology* 178: 295–312.

ENGLAND, W. H., AND R. J. TOLBERT. 1964. A seasonal study of the vegetative shoot apex of *Myriophyllum heterophyllum*. *American Journal of Botany* 51: 349–353.

ERICKSON, R. O. 1983. The geometry of phyllotaxis. *In* J. E. Dale and F. L. Milthrope [eds.], The growth and functioning of leaves, 53–88. University Press, Cambridge, UK.

ESAU, K. 1965. Plant anatomy, 2nd ed. John Wiley & Sons, New York, New York, USA.

GIFFORD, E. M. 1943. The structure and development of the shoot apex of *Ephedra altissima*. *Bulletin of the Torrey Botanical Club* 70: 15–25.

GIFFORD, E. M. 1954. The shoot apex in angiosperms. *Botanical Review* 20: 477–529.

GIFFORD, E. M., AND A. S. FOSTER. 1989. Morphology and evolution of vascular plants, 3rd ed. W. H. Freeman, New York, New York, USA.

GLEASON, H. A., AND A. CRONQUIST. 1991. Manual of vascular plants of northeastern United States and adjacent Canada, 2nd ed. New York Botanical Garden, Bronx, New York, USA.

GREEN, P. B. 1999. Expression of pattern in plants: combining molecular and calculus-based biophysical paradigms. *American Journal of Botany* 86: 1059–1076.

GREEN, P. B., C. S. STEELE, AND S. C. RENNICH. 1996. Phyllotactic patterns; a bio-physical mechanism for their origin. *Annals of Botany* 77: 515–527.

GREYSON, R. I., D. B. WALDEN, AND J. A. HUME. 1978. The ABPHYL syndrome in *Zea mays*. II. Patterns of leaf initiation and the shape of the shoot meristem. *Canadian Journal of Botany* 56: 1545–1550.

HEYWOOD, V. H. 1993. Flowering plants of the world, updated edition. Oxford University Press, New York, New York, USA.

ITOH, J., A. HASEGAWA, H. KITANO, AND Y. NAGATO. 1998. A recessive heterochronic mutation, *plastochron1,* shortens the plastochron and elongates the vegetative phase in rice. *Plant Cell* 10: 1511–1521.

ITOH, J., H. KITANO, M. MATSUOKA, AND Y. NAGATO. 2000. SHOOT ORGANIZATIONgenes regulate shoot apical meristem organization and the pattern of leaf primordium initiation in rice. *Plant Cell* 12: 2161–2174.

JEAN, R. V. 1992. On the origins of spiral symmetry in plants. *In* I. Hargittai [ed.], Spiral symmetry, 323–351. World Scientific, Singapore, China.

JEAN, R. V. 1994. Phyllotaxis, a systematic study in plant morphogenesis. Cambridge University Press, New York, New York, USA.

JEAN, R. V., and D. Barbabe. 1998. Symmetry in plants. World Scientific, River Edge, New Jersey, USA.

KAPLAN, D. R. 2001. The science of plant morphology: definition, history, and role in modern biology. *American Journal of Botany* 88: 1711–1741.

KAPLAN, D. R., AND T. J. COOKE. 1997. Fundamental concepts in the embryogenesis of dicotyledons: a morphological interpretation of embryo mutants. *Plant Cell* 9: 1903–1919.

KOLLER, D., H. R. HIGHKIN, AND O. H. CASO. 1960. Effects of gibberellic acid on stem apices of vernalizable grasses. *American Journal of Botany* 47: 518–524.

KWIATKOWSKA, D. 1999. Formation of pseudowhorls in *Peperomia verticillata* (L.) A. Dietr. shoots exhibiting various phyllotactic patterns. *Annals of Botany* 83: 675–685.

LEYSER, H. M. O., AND I. J. FURNER. 1992. Characterization of three shoot apical meristem mutants of *Arabidopsis thaliana*. *Development* 116: 397–403.

LYNDON, R. F. 1998. The shoot apical meristem: its growth and development. Cambridge University Press, Cambridge, UK.

MATSUO, T., AND K. HOSHIKAWA. 1993. Science of the rice plant, vol. 1. Morphology. Food & Agriculture Policy Research Center, Tokyo, Japan.

MCCULLY, M. E., AND H. M. DALE. 1961. Variations in leaf number in *Hippuris*. A study of whorled phyllotaxis. *Canadian Journal of Botany* 39: 611–625.

MEINHARDT, H. 1982. Models of biological pattern formation. Academic Press, London, UK.

MITCHISON, G. H. 1977. Phyllotaxis and the Fibonacci series. *Science* 196: 270–275.

NAGASAWA, N., M. MIYOSHI, H. KITANO, H. SATOH, AND Y. NAGATO. 1996. Mutations associated with floral organ number in rice. *Planta* 198: 627– 633.

NIKLAS, K. J. 1998. Light harvesting ‘‘fitness landscapes’’ for vertical shoots with different phyllotactic patterns. *In* R. V. Jean and D. Barabe [eds.], Symmetry in plants, 759–773. World Scientific, River Edge, New Jersey, USA.

O’BRIEN, T. P., AND M. E. MCCULLY. 1969. Plant structure and development, a pictorial and physiological approach. MacMillan, New York, New York, USA.

PAOLILLO, D. J., JR., AND E. M. GIFFORD, JR. 1961. Plastochronic changes and the concept of the apical initials in *Ephedra altissima*. *American Journal of Botany* 48: 8–16.

QUI, Y., J. LEE, B. A. WHITLOCK, F. BERNASCONI-QUADRONI, AND O. DOMBROVSKA.2001. Was the ANITA rooting of the angiosperm phylogeny affected by long-branch attraction? *Molecular Biology and Evolution* 18: 1745–1753.

RUTISHAUSER, R. 1984. Blattquirle, Stipeln und Kolleteren bei den *Rubieae* (Rubiaceae) im Vergleich mit anderen Angiospermen. *Beitra¨ge zur Biologie der Pflanzen* 59: 375–424.

RUTISHAUSER, R., AND R. SATTLER. 1987. Complementarity and heuristic value of contrasting models in structural botany. II. Case study on leaf whorls: *Equisetum* and *Ceratophyllum*. *Botanische Jahrbu¨cher fur Systematik, Pflanzengeschichte und Pflanzengeographie* 109: 227–255.

SAM, S. J. 1984. The structure of the apical meristem of *Isoetes engelmannii*, *I. Riparis* and *I. Macrospora* (Isoetales). *Botanical Journal of the Linnean*
SAVELKOUL, R. M. H. 1957. Distribution of mitotic activity within the shoot apex of *Elodea densa*. *American Journal of Botany* 44: 311–317.

SCHMIDT, B. L., AND W. F. MILLINGTON. 1968. Regulation of leaf shape in *Proserpinaca palustris*. *Bulletin of the Torrey Botanical Club* 95: 264– 286.

SCHOUTE, J. C. 1921. On whorled phyllotaxis. I. Growth whorls. *Recueil des travaux Botaniques Ne´erlandais* 19: 184–206
.
SCHOUTE, J. C. 1925. On whorled phyllotaxis. II. Late binding whorls of *Peperomia*. *Recueil des travaux Botaniques Ne´erlandais* 22: 128–172.

SCHOUTE, J. C. 1936. On whorled phyllotaxis. III. True and false whorls. *Recueil des travaux Botaniques Ne´erlandais* 33: 670–687.

SCHOUTE, J. C. 1938. On whorled phyllotaxis. IV. Early binding whorls. *Recueil des travaux Botaniques Ne´erlandais* 35: 415–558.

SCULTHORPE, C. D. 1967. The biology of aquatic vascular plants. Edward Arnold, London, UK.

SHARMAN, B. C. 1945. Leaf and bud initiation in the Gramineae. *Botanical Gazette* 106: 269–289.

STERLING, C. 1949. The primary body of the shoot of *Dianthera americana*. *American Journal of Botany* 36: 184–193.

SUN, G., Q. JI, D. L. DILCHER, S. ZHENG, K. C. NIXON, AND X. WANG. 2002. Archaefructaceae, a new basal angiosperm family. *Science* 296: 899– 904.

TAKEDA, H. 1916. Some points in the morphology of the stipules in the Stellatae, with special reference to Galium. *Annals of Botany* 30: 199– 214.

TAMURE, Y., K. HIDEMI, S. HIKARU, AND N. YASUO. 1992. A gene profoundly affecting shoot organization in the early phase of rice development. *Plant Science* 82: 91–99.

THORNLEY, J. H. M. 1975. Phyllotaxis. I. A mechanistic model. *Annals of Botany* 39: 491–507.

TROLL, W. 1943. Vergleichende Morphologie der ho¨heren Pflanzen. Erster Bankd: Vegetationsorgane. Teil III. Gebru¨der Borntraeger, Berlin, Germany.

VEEN, A. H., AND A. LINDENMAYER. 1977. Diffusion mechanism for phyllotaxis: theoretical physico-chemical and computer study. *Plant Physiology* 60: 127–139.

WATSON, L., AND M. J. DALLWITZ. 2000. The families of flowering plants: descriptions, illustrations, identification, and information retrieval. Version: 14 December 2000. http://biodiversity.uno.edu/delta/.

WILLIAMS, R. F. 1975. The shoot apex and leaf growth a study in quantitative biology. Cambridge University Press, New York, New York, USA.

WILLIAMS, R. F., AND R. A. METCALF. 1985. The genesis of form in Casuarinaceae. *Australian Journal of Botany* 33: 563-578.

WILLIAMS, R. F., R. A. METCALF, AND L. W. GUST. 1982. The genesis of form in Oleander (*Nerium oleander* L.). *Australian Journal of Botany* 30: 677–687.

ZOMLEFER, W. B. 1994. Guide to flowering plant families. University of North Carolina Press, Chapel Hill, North Carolina, USA.